

This article was downloaded by:

On: 25 January 2011

Access details: *Access Details: Free Access*

Publisher *Taylor & Francis*

Informa Ltd Registered in England and Wales Registered Number: 1072954 Registered office: Mortimer House, 37-41 Mortimer Street, London W1T 3JH, UK



Separation Science and Technology

Publication details, including instructions for authors and subscription information:

<http://www.informaworld.com/smpp/title~content=t713708471>

Gaseous Pollutant Removal by a Single Bed Cyclic Adsorber with Synchronous Thermal Contact

H. H. Hsu^a; K. B. Wang^a; L. T. Fan^a

^a DEPARTMENT OF CHEMICAL ENGINEERING, KANSAS STATE UNIVERSITY, MANHATTAN, KANSAS

To cite this Article Hsu, H. H. , Wang, K. B. and Fan, L. T.(1976) 'Gaseous Pollutant Removal by a Single Bed Cyclic Adsorber with Synchronous Thermal Contact', *Separation Science and Technology*, 11: 2, 109 — 132

To link to this Article: DOI: 10.1080/01496397608085306

URL: <http://dx.doi.org/10.1080/01496397608085306>

PLEASE SCROLL DOWN FOR ARTICLE

Full terms and conditions of use: <http://www.informaworld.com/terms-and-conditions-of-access.pdf>

This article may be used for research, teaching and private study purposes. Any substantial or systematic reproduction, re-distribution, re-selling, loan or sub-licensing, systematic supply or distribution in any form to anyone is expressly forbidden.

The publisher does not give any warranty express or implied or make any representation that the contents will be complete or accurate or up to date. The accuracy of any instructions, formulae and drug doses should be independently verified with primary sources. The publisher shall not be liable for any loss, actions, claims, proceedings, demand or costs or damages whatsoever or howsoever caused arising directly or indirectly in connection with or arising out of the use of this material.

Gaseous Pollutant Removal by a Single Bed Cyclic Adsorber with Synchronous Thermal Contact

H. H. HSU, K. B. WANG, and L. T. FAN

DEPARTMENT OF CHEMICAL ENGINEERING

KANSAS STATE UNIVERSITY

MANHATTAN, KANSAS 66506

Abstract

A single fixed bed pollutant adsorber can be operated cyclically by synchronizing the change of the direction of the gaseous flow with the change of the temperature in the bed. The pollutant is adsorbed at a temperature lower than that at which it is desorbed. The desorbed pollutant is then burned and disposed of.

Two operational schemes are presented for such a system. Effects of several parameters on the adsorber performance are studied through computer simulation. The results of this study can serve as a guideline in designing such a single bed adsorber system.

INTRODUCTION

The adsorption process has been employed mostly in the separation of fluids and solvent recovery (18). The adsorption process has also been increasingly employed for pollutant removal from air (7). An adsorption unit usually consists of one, two, or more fixed-bed adsorbers (5, 16). To remove the pollutant (the adsorbate), a pollutant laden air stream can be passed through an adsorbent-packed bed or beds wherein the pollutant is concentrated. The adsorption process is continued until the effluent stream from the bed reaches the threshold or maximum allowable concentration. At this point the concentrated pollutant must be disposed of. The disposal of the pollutant may be effected in any of the following ways: (a) the ad-

sorbent along with the pollutant is discarded, (b) the pollutant is desorbed and either recovered, if it contains valuable components, or discarded, or (c) the pollutant is oxidized on the adsorbent surface and removed.

Among the methods of disposing of the concentrated pollutant, the on-site (or in-system) desorption which gives rise to a cyclic operation appears to be the most practical because this method has the following advantages over other methods: (a) no handling of solids is needed during operation, (b) no replacement of the adsorber is necessary, and (c) the adsorption-desorption cycles are repeated continuously. The last point is of particular importance for those situations where the pollutant is continuously generated. To achieve a continuous cyclic operation, usually two or more adsorber beds are used (14, 16). However, as is shown in this paper, a single bed adsorber can also handle the continuous pollutant flow effectively. The primary aim of the present study is to show the feasibility of such a single bed adsorber-desorber system (or simply single bed adsorber system) and understand its performance through computer simulation. Such a compact system can be installed in restaurants, laundries, foundries, laboratories, painting rooms, workshops, mines, etc. It can also find application in space ships and submarines due to its compact character.

Cyclic adsorption-desorption processes for fluid separation have been studied by several investigators. Wilhelm et al. (19, 20) and Sweed and Wilhelm (17) first introduced the concept of parametric pumping. Parametric pumping is a cyclic separation process in which two synchronous actions—a periodic temperature variation and an alternating fluid flow—are imposed on a bed of adsorbent. The alternating fluid flow through the adsorber is coupled with cycling of temperature levels, thus causing a build-up of separation from cycle to cycle. Such a system is a closed system in which the fluid mixture flows between two reservoirs at two opposite ends of the adsorber. There is neither feed introduced nor product withdrawn during the cycles until the separation is complete. This is equivalent to a batch process. Gregory and Sweed (8, 9) and Chen et al. (3, 4) later modified it by continually introducing the feed and withdrawing the product during portions of a cycle. As for the mathematical model of the adsorption process, Pigford et al. (15) assumed an equilibrium theory while Gupta and Sweed (10) presented a more realistic nonequilibrium theory. Recently, Kowler and Kadlec (12) considered the separation of a gaseous mixture in a fixed bed adsorber by cyclically regulating the pressure gradients in the bed. For the pollution control oriented adsorption system

presented here, some operational schemes based on a concept similar to parametric pumping with thermal contact are incorporated. These schemes are to be arranged so that the continuous flow of the pollutant laden air stream is possible.

The desorbed pollutant may be scrubbed by water or it can be burned and disposed of. Since water scrubbing usually requires a large scrubbing tower and may cause water pollution (7), it is not desirable for the compact system under consideration. In the present system the desorbed pollutant is burned into harmless gases and thus an incinerator is included in the system.

In the following, the operational schemes of the system under consideration are first described. The mathematical model for the adsorber is then formulated, and the effects of some significant parameters on the performance of the system are investigated by computer simulations.

OPERATIONAL SCHEMES

Two operational schemes are proposed here. One uses fresh air for desorption and the other uses exhaust gas, as shown in Figs. 1 and 2, respectively. The adsorber is packed with a bed of activated carbon. Activated carbon is used as adsorbent because it is very effective in adsorbing different organic molecules, even from a humid gas stream (11, 16). The adsorber is embedded with a coiled tube for cooling or heating purposes. (Alternatively, the adsorber can be embedded with parallel tubes in a manner similar to a shell and tube heat exchanger.) It is assumed that the temperature in the bed can be kept uniform by means of the tube (or tubes). The jacketed incinerator is used to burn the pollutant during the desorption period, and it also serves as a heat exchanger.

At the beginning of a cycle, the adsorber bed is cooled to a desirable temperature by flowing a cool fresh air stream or cold water through the coiled tube as shown in Figs. 1 and 2. While the bed is kept cool, the pollutant laden air stream (henceforth called feed) flows through the bed from top to bottom. Initially, the adsorbent is relatively clean so that the pollutant is almost completely adsorbed. Consequently, the effluent air stream is virtually free of the pollutant and can be ejected to the atmosphere. As adsorption continues, the adsorbent becomes increasingly saturated and the pollutant concentration in the effluent stream increases gradually. When the effluent concentration reaches the maximum allowable concentration, the adsorption process is interrupted and the system is switched

Scheme I

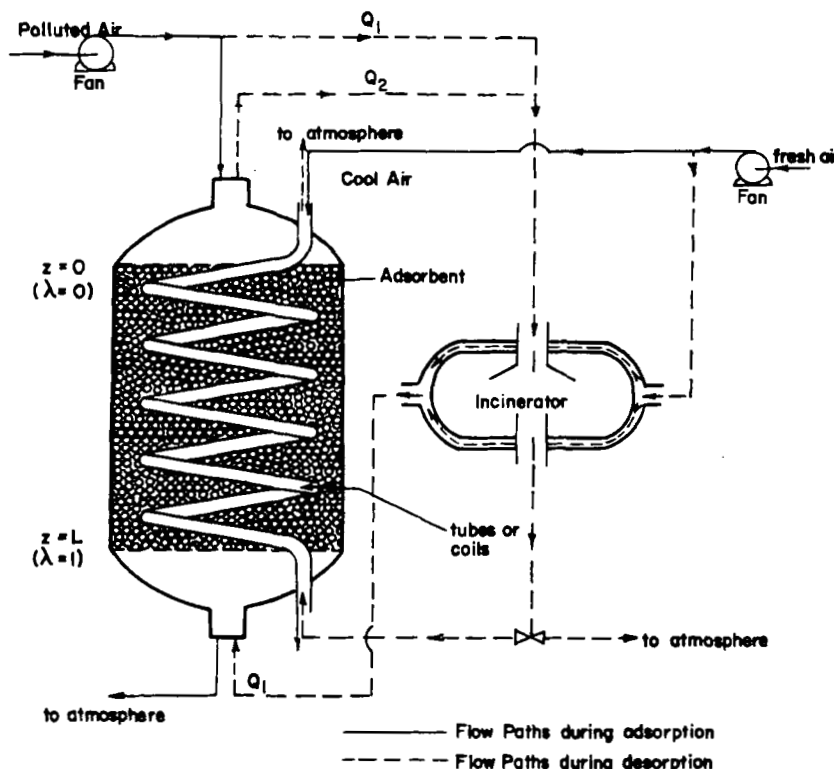


FIG. 1. A single adsorber system using fresh air for desorption.

to the desorption phase. A plot of the effluent pollutant concentration vs time is called a breakthrough curve and is illustrated in Fig. 3 where c_f is the feed concentration and c_{\max} is the maximum allowable concentration. Thus, when the effluent concentration reaches c_{\max} , the feed is diverted to the incinerator where it is burned together with the desorbed pollutant. It is assumed that the capacity of the incinerator is large enough so that the pollutant can be burned almost completely. Thus the exhaust from the incinerator is free of the pollutant.

The desorption process can be effected by two different schemes. These are distinguished as Scheme I in Fig. 1 and Scheme II in Fig. 2. In Scheme

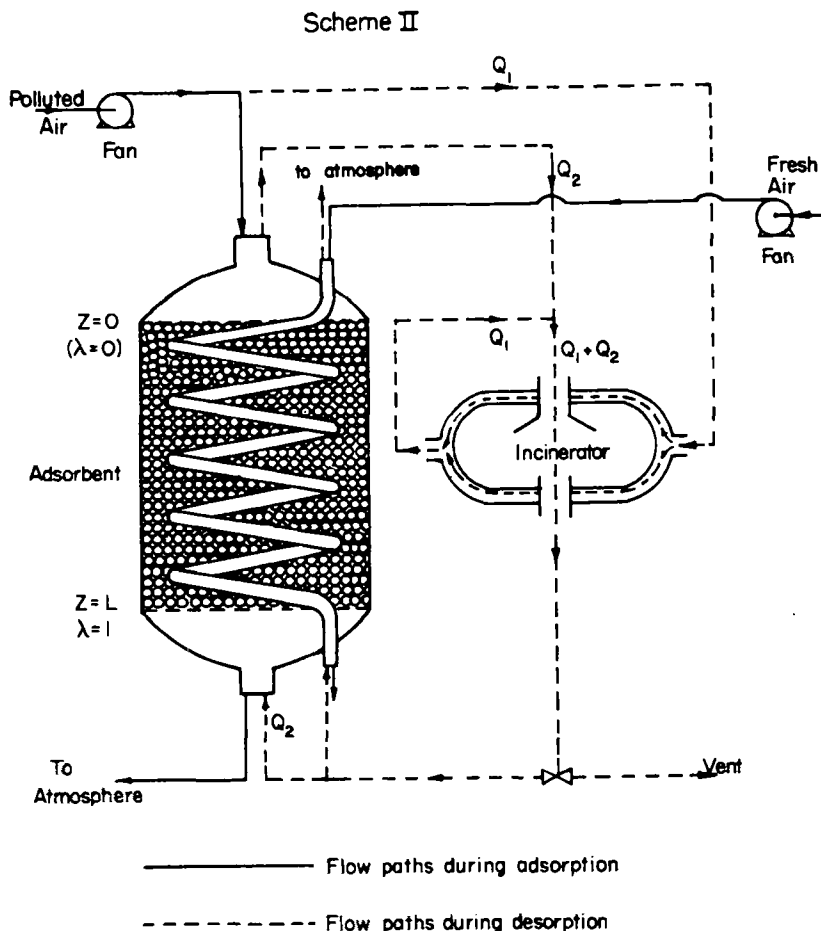


FIG. 2. A single adsorber system using exhausted air for desorption.

I a portion of the exhaust gas from the incinerator is allowed to flow through the coiled tube to raise the bed temperature. At the same time a fresh air stream flows through the jacket of the incinerator. The heated fresh air stream then flows upward through the bed to desorb the pollutant. The desorbed pollutant stream combines with the original pollutant laden stream before entering the incinerator. The desorption process is stopped when the bed has been cleaned to a certain level (this point will be detailed

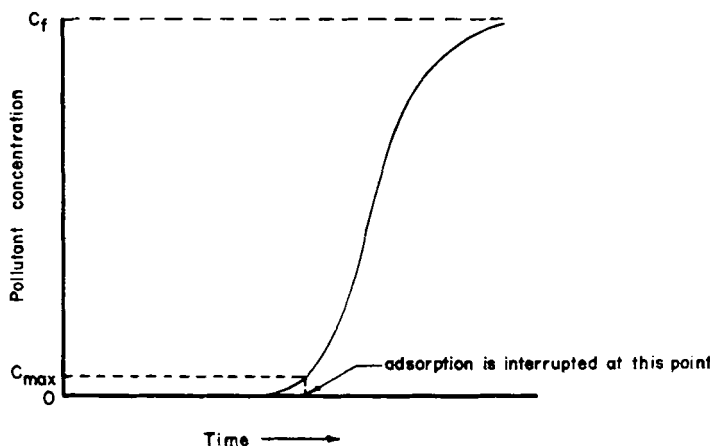


FIG. 3. Schematic of a typical breakthrough curve.

later). This completes one adsorption-desorption cycle. Thus, within a cycle, the direction of flow is changed synchronously with the change of bed temperature.

Scheme II is a modification of Scheme I. It differs from Scheme I in that it does not require an additional fresh air stream for desorption. The exhaust gas stream from the incinerator is divided into two streams; one is used to heat the adsorber through the coiled tube and the other to desorb the pollutant. Since it is assumed that the exhaust gas is essentially free of pollutant, it can be considered as an inert gas and thus has the same desorbing property as fresh air. Note that the feed stream is heated in the incinerator jacket before it combines with the desorbed polluted stream. Thus the heat loss due to mixing is reduced.

In comparing the two schemes described above, it appears that Scheme II is more advantageous than Scheme I because no additional air stream is required and heat loss due to mixing is reduced. Furthermore, in Scheme II an inert gas is used for desorption. This can prevent the activated carbon in the bed from being oxidized. Scheme II, however, does have some disadvantages. The stream entering the incinerator is diluted due to mixing of the desorbed stream with the feed stream (see Fig. 2), and this dilution may require excessive thermal energy for incineration of the pollutant. Moreover, if the exhaust gas from the incinerator contains a substantial amount of particulates, the exhaust gas stream should pass a filter before entering the adsorber.

MATHEMATICAL MODEL OF THE ADSORBER

The assumptions made in deriving the performance equations of the single adsorber system under consideration are:

- (a) The adsorption process takes place isothermally at a lower temperature and the desorption process takes place isothermally at a higher temperature.
- (b) External mass transfer is the rate-controlling step. The model of mass transfer based on this assumption is called the film model (6).
- (c) Parameters such as mass transfer coefficient, porosity of bed, adsorbent density, and specific surface area of adsorbent do not change with respect to operating conditions.
- (d) No dispersion of the gaseous components occurs in the entrance and exit sections adjacent to the bed, although the existence of dispersion within the bed is not neglected.

Under these assumptions the following differential equations can be written by taking mass balances on the adsorbate and the adsorbent:

$$H_g \frac{\partial c}{\partial t} = \epsilon \rho_g D \frac{\partial^2 c}{\partial z^2} \mp G \frac{\partial c}{\partial z} - k_e a \rho_g (c - c^*) \quad (1)$$

$$H_s \frac{\partial q}{\partial t} = k_e a \rho_g (c - c^*) \quad (2)$$

The ambiguous sign in Eq. (1) accounts for the direction of the gaseous flow. The positive direction is that from top to bottom. In other words, the positive direction in the bed is always measured from the top. Thus, the “-” should be used during adsorption while the “+” should be used during desorption. In Eqs. (1) and (2), c^* is the gas phase equilibrium concentration which is related to q by a Langmuir-type isotherm

$$q = \frac{q_m b c^*}{1 + b c^*} \quad (3)$$

where q_m is the amount of adsorbate on unit mass of adsorbent when the adsorbent is fully covered by a monolayer of the adsorbate. The constant b is determined from (2)

$$b = \frac{A_1 \exp(A_2/T)}{T^{1/2}} \quad (4)$$

where A_1 and A_2 are constants and T is the temperature of the adsorber bed.

Let the overall time or period of each cycle be t_c , the adsorption time t_a , and the desorption time t_d . It is assumed that the switching from adsorption to desorption is instantaneous so that $t_c = t_a + t_d$. Because of the cyclic steady-state nature of the operation, the initial conditions of the adsorption process are those at the end of the desorption and vice versa. These conditions, along with the appropriate boundary conditions for Eqs. (1) and (2), can be expressed mathematically as shown below, noting that the directions of flow are opposite to each other during the adsorption and desorption processes.

During adsorption

$$c(0, z) = c(t_c^-, L - z) \quad (5)$$

$$q(0, z) = q(t_c^-, L - z) \quad (6)$$

$$c(t, 0) = c_f + \frac{\varepsilon \rho_g D}{G} \frac{\partial c(t, 0)}{\partial z} \quad \left. \right\} \quad 0 \leq t \leq t_a^- \quad (7)$$

$$\frac{\partial c(t, L)}{\partial z} = 0 \quad \left. \right\} \quad (8)$$

During desorption

$$c(t_a^+, z) = c(t_a^-, L - z) \quad (9)$$

$$q(t_a^+, z) = q(t_a^-, L - z) \quad (10)$$

$$c(t, L) = c^d - \frac{\varepsilon \rho_g D}{G} \frac{\partial c(t, L)}{\partial z} \quad \left. \right\} \quad t_a^+ \leq t \leq t_c^- \quad (11)$$

$$\frac{\partial c}{\partial z}(t, 0) = 0 \quad \left. \right\} \quad (12)$$

In the above equations, c^d is the inlet concentration of the pollutant in the desorbing air stream. For either scheme, c^d is zero since the desorbing stream contains no pollutant. t_a^- indicates the end of the adsorption period, t_a^+ the beginning of the desorption period, and t_c^- the end of the desorption period. The temperature, T , in Eq. (4) is T_a for adsorption and T_d for desorption.

Equations (1) through (12) can be rewritten in dimensionless forms by introducing the following dimensionless quantities.

$$X = c/c_f$$

$$Y = q/q_m$$

$$\lambda = z/L$$

$$\tau = tG/LH_g$$

$$Pe = GL/\epsilon \rho_g D$$

$$K_e = k_e a \rho_g L/G$$

$$\alpha = H_g c_f / H_s q_m$$

$$B = bc_f$$

The resulting governing equations are

$$\frac{\partial X}{\partial \tau} = \frac{1}{Pe} \frac{\partial^2 X}{\partial \lambda^2} \mp \frac{\partial X}{\partial \lambda} - K_e (X - X^*) \quad (13)$$

$$\frac{\partial Y}{\partial \tau} = K_e (X - X^*) \quad (14)$$

where X^* is determined from the equilibrium condition

$$Y = \frac{BX^*}{1 + BX^*} \quad (15)$$

The corresponding dimensionless initial and boundary conditions are, during adsorption,

$$X(0, \lambda) = X(\tau_c^-, 1 - \lambda) \quad (16)$$

$$Y(0, \lambda) = Y(\tau_c^-, 1 - \lambda) \quad (17)$$

$$X(\tau, 0) = 1 + \frac{1}{Pe} \frac{\partial X(\tau, 0)}{\partial \lambda} \quad (18)$$

$$\frac{\partial X(\tau, 1)}{\partial \lambda} = 0 \quad (19)$$

and during desorption,

$$X(\tau_a^+, \lambda) = X(\tau_a^-, 1 - \lambda) \quad (20)$$

$$Y(\tau_a^+, \lambda) = Y(\tau_a^-, 1 - \lambda) \quad (21)$$

$$X(\tau, 1) = - \frac{1}{Pe} \frac{\partial X(\tau, 1)}{\partial \lambda} \quad (22)$$

$$\frac{\partial X(\tau, 0)}{\partial \lambda} = 0 \quad (23)$$

Equations (13) through (15) together with Eqs. (16) through (23) cannot be solved analytically because of the nonlinearity appearing in Eq. (15). They can be solved, however, by the finite difference method (1). It should be noted that the solutions for Schemes I and II are identical although there is a practical difference in operation between the two schemes as described previously.

RESULTS OF SIMULATION AND DISCUSSION

The performance of the adsorber system under consideration is examined with respect to significant parameters such as:

- (a) Pollutant concentration in the feed.
- (2) Maximum allowable concentration.
- (3) Adsorption temperature.
- (4) Desorption temperature.
- (5) Linear velocity of the gas flow.
- (6) Residual pollutant loading at the end of desorption.
- (7) Extent of the axial dispersion characterized by the Peclet number.

The first parameter depends on the content of a pollution source. The second parameter is related to human tolerance toward the pollutant and is usually regulated by emission standards. The other parameters are subject to a designer's choice. Thus it is desirable to examine the effects of each parameter on the system's performance. As a basis for comparison, the results of simulation for a set of nominal values of the parameters are first presented and discussed. The effects of each parameter are analyzed subsequently.

The numerical values of the nominal conditions are listed in Table 1.

TABLE 1
Numerical Values of Nominal Conditions

(1)	c_f , feed concentration	500 ppm
(2)	c_{max} , maximum allowable concentration	25 ppm
(3)	T_a , adsorption temperature	25°C
(4)	T_d , desorption temperature	70°C
(5)	P , pressure in the adsorber	1 atm
(6)	u , superficial linear velocity of gaseous flow	40 cm/sec
(7)	β , residual pollutant loading at the end of desorption	5%
(8)	Pe, Peclet number	200

TABLE 2
Additional Constants Employed in the Simulation

$a = 15 \text{ cm}^2/\text{cm}^3$
$A_1 = 0.2312 \times 10^{-3} (\text{°K})^{1/4}$
$A_2 = 0.44076 \times 10^4 \text{ °K}$
$D_a = 30 \text{ cm}$
$d_p = 0.4 \text{ cm}$
$k_e = 3 \text{ cm/sec}$
$L = 40 \text{ cm}$
$q_m = 0.5 \text{ g/g}$
$\epsilon = 0.4$
$\rho_s = 0.75 \text{ g/cm}^3$

Additional constants employed in the simulation are listed in Table 2. Under these conditions, the dimensionless quantities K_e and α are,

For adsorption: $K_e = 45.0$

$$\alpha = 1.046 \times 10^{-6}$$

For desorption: $K_e = 37.46$

$$\alpha = 8.71 \times 10^{-7}$$

In this study the direction of flow during desorption is opposite to that during adsorption. This is due to the fact that at the end of adsorption, a pollutant concentration gradient exists in the bed where the upper portion is almost saturated while the lower portion is relatively clean. If desorption were conducted in the same direction, some of the pollutant which has been desorbed from the upper portion would be readsorbed in the lower portion, thereby hindering the desorption process. If desorption were conducted in the opposite direction, this phenomenon would not occur.

Figures 4 and 5 show the distributions of the pollutant concentrations in the gas and solid phases, respectively, during the adsorption period. It can be seen that at the early stage of adsorption, only a narrow zone near the top end is contaminated. As the period of time increases, the pollutant concentrations in both the gas and solid phases increase at every point. Of particular interest is the increase in the gas phase at the exit ($\lambda = 1$) as shown in Fig. 6. The effluent concentration is essentially free of pollutant for approximately 26 min, after which it increases very sharply. As soon as the maximum allowable concentration (in this case, 25 ppm) is reached, the

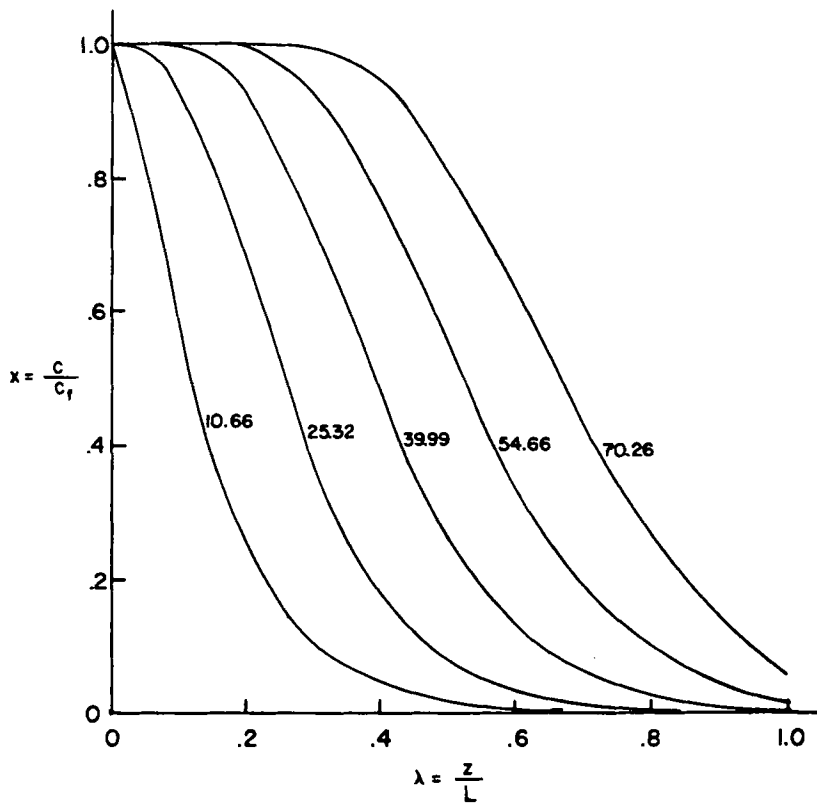


FIG. 4. Gas phase pollutant concentration during adsorption period (nominal conditions, parameters; time, minutes).

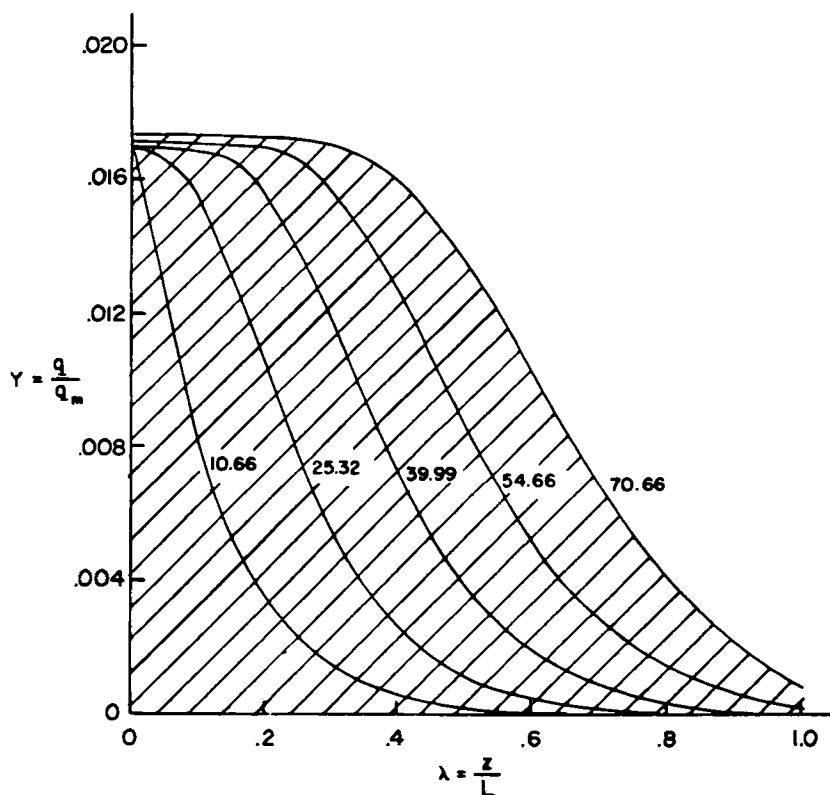


FIG. 5. Solid phase pollutant concentration during adsorption period (nominal conditions, parameters; time, minutes).

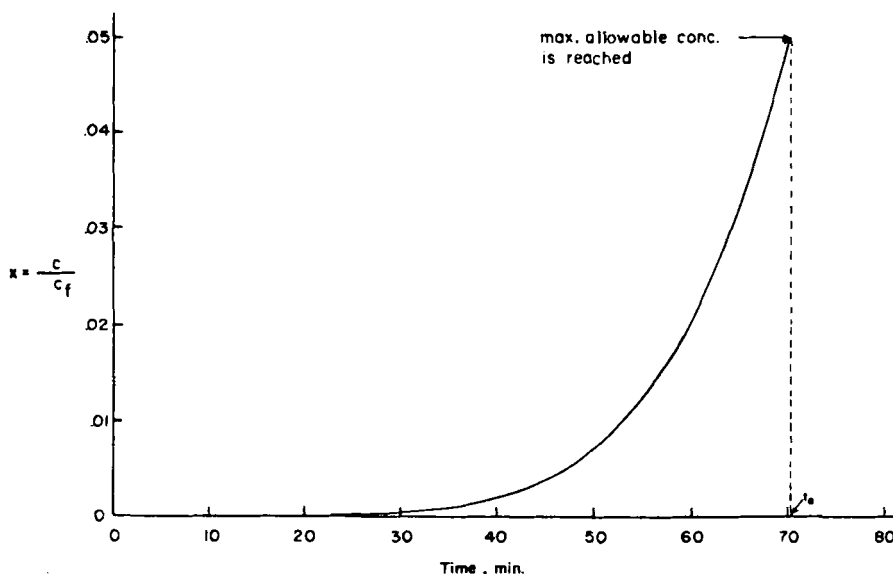


FIG. 6. Effluent pollutant concentration during adsorption period (nominal conditions).

adsorption operation is interrupted. The amount of pollutant loaded on the adsorbent can be obtained by integrating

$$Q_1 = \rho_s (1 - \varepsilon) q_m A L \int_0^1 Y_{fA} d\lambda \quad (24)$$

where Y_{fA} is the solid phase pollutant concentration profile at the termination of adsorption. Note that the quantity

$$\int_0^1 Y_{fA} d\lambda$$

is represented by the shaded area in Fig. 5.

As soon as adsorption is terminated, desorption is initiated. During the desorption operation the pollutant concentrations in the gas and solid phases decrease as shown in Figs. 7 and 8, respectively. Since the desorbing air stream flows upward, the pollutant is desorbed faster in the lower part (larger λ) than in the upper part (smaller λ). Desorption is terminated when the residual pollutant loading on the adsorbent is at a certain fraction (in the nominal case, 5%) of the original loading, i.e., Q_1 . The amount of the

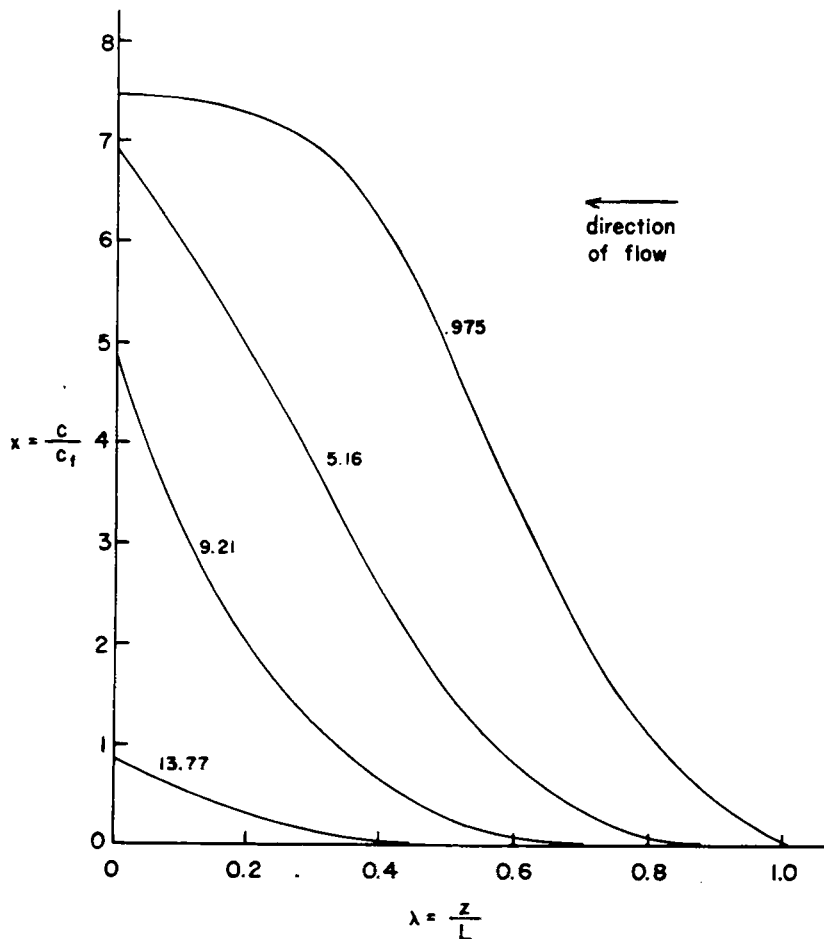


FIG. 7. Gas phase pollutant concentration during desorption period (nominal conditions, parameters; time, minutes).

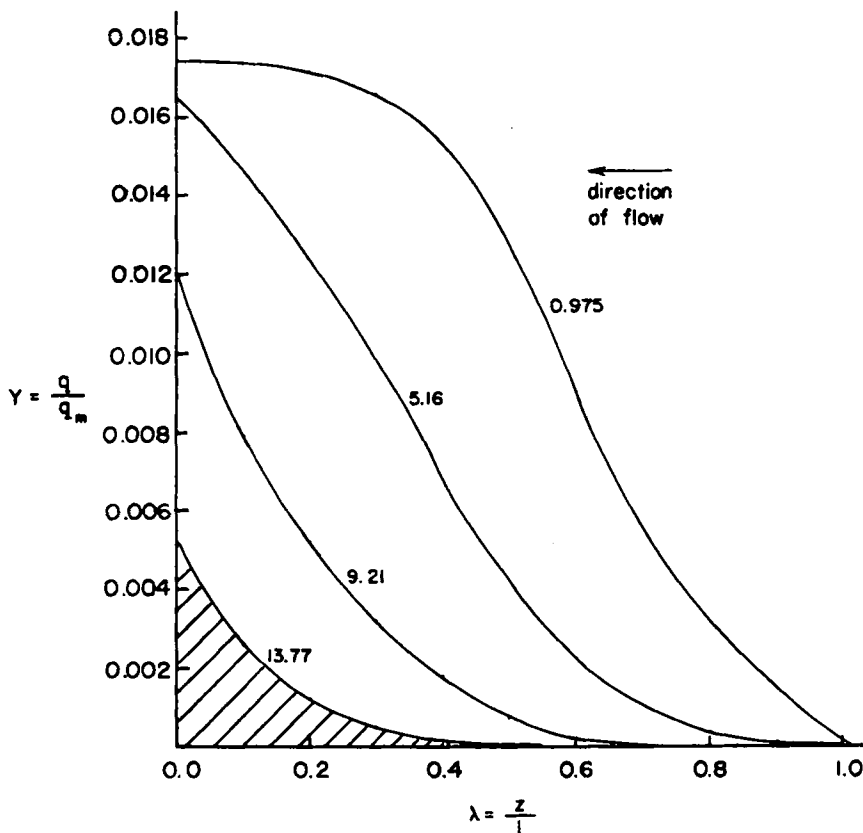


FIG. 8. Solid phase pollutant concentration during desorption period (nominal conditions, parameters; time, minutes).

residual pollutant on the adsorbent can be obtained as

$$Q_2 = \rho_s(1 - \varepsilon)q_m A L \int_0^1 Y_{fD} d\lambda \quad (25)$$

where Y_{fD} is the solid phase pollutant concentration profile at the end of desorption. As before, the quantity

$$\int_0^1 Y_{fD} d\lambda$$

is represented by the shaded area in Fig. 8.

TABLE 3
Effects of Various Parameters on Adsorber Performance

No.	Parameters						Adsorption time (min)	Desorption time (min)	Fraction of desorption operation	Capacity of adsorption (g/cycle)	Removal rate of adsorber (g/min)
	c_f (ppm)	c_{max} (ppm)	T_a (°C)	T_d (°C)	P (atm)	u (cm/sec)					
1	500	25	25	70	1	40	5	200	70.3	13.8	0.164
2	500	25	25	70	1	40	5	200	79.5	14.6	0.155
3	500	25	25	70	1	40	5	200	62.5	13.0	0.172
4	500	25	25	70	1	40	5	200	60.5	12.7	0.173
5	500	25	25	70	1	40	5	200	79.3	14.6	0.155
6	500	25	25	70	1	40	5	200	89.4	13.6	0.132
7	500	25	25	70	1	40	5	200	55.7	14.0	0.201
8	500	25	25	70	1	40	5	200	70.3	20.5	0.226
9	500	25	25	70	1	40	5	200	70.3	9.5	0.119
10	500	25	25	70	1	40	5	200	140.7	27.2	0.162
11	500	25	25	70	1	40	5	200	35.2	6.8	0.162
12	500	25	25	70	1	40	5	200	98.3	18.1	0.155
13	500	25	25	70	1	40	5	200	53.7	11.2	0.173
14	500	25	25	70	1	40	1	200	75.1	17.6	0.190
15	500	25	25	70	1	40	10	200	63.9	11.7	0.155
16	500	25	25	70	1	40	5	100	65.2	13.2	0.168
17	500	25	25	70	1	40	5	83.6	19.8	0.191	78.9
											0.763

The capacity of adsorption per cycle is defined as the difference between the original loading and the residual loading. Let the capacity be denoted by ΔQ . Then

$$\Delta Q = Q_1 - Q_2 \quad (26)$$

This quantity divided by the time of a cycle gives the pollutant removal rate of the adsorber. The adsorption time or period, desorption time, capacity per cycle, and removal rate of the adsorber along with the values of the parameters are tabulated in Table 3. These values for the nominal case are contained in the first row. Starting from the second row, one parameter each is varied from the nominal values. The values which deviate from the nominal values are encircled.

The effects of the various parameters on the adsorber performance are discussed in what follows.

Feed Concentration

The results in Table 3 show that the removal rate of the adsorber is almost proportional to the feed concentration. However, the cycle time decreases with increasing feed concentration but the fraction of time for the desorption operation increases with increasing feed concentration. Hence a higher feed concentration needs more frequent desorption. Furthermore, a higher feed concentration is usually achieved by applying pressure. Higher pressure in the adsorber not only increases the power cost but also adds construction costs. Therefore, a higher feed concentration has no advantage for the cyclic operation.

The mathematical model is simulated for two different feed concentrations, one lower and one higher than the nominal values, keeping all other parameters unchanged. The results are presented in row 2 and row 3, respectively, of Table 3. It is obvious that if the feed concentration is lower, the pollutant removal rate is lower, and vice versa.

Maximum Allowable Concentration

As mentioned previously, the maximum allowable concentration is usually regulated by local emission standards. If a stricter emission standard is imposed on the system, the maximum allowable concentration, c_{max} , should be lowered. Conversely, if the emission standard is slackened, c_{max} can be increased.

The pollutant removal rates for different values of c_{max} are almost identi-

cal. However, the cycle time increases with increasing c_{max} , but the fraction of time for desorption operation decreases with increasing c_{max} . The results from the effect of this parameter are given in rows 4 and 5 of Table 3. It is interesting to note that the pollutant removal rates for different values of c_{max} are almost identical although the adsorption time, desorption time, and adsorption capacities vary significantly.

Adsorption Temperature

At 20, 25, and 30°C, the adsorption times are 89.4, 70.3, and 55.7 min, respectively. These results indicate that the adsorption process is very sensitive to the adsorption temperature. The cycle time increases with a decrease in adsorption temperature, but the fraction of time for the desorption operation decreases with decreasing adsorption temperature. Moreover, the lower the adsorption temperature the higher the removal rate of adsorber. Therefore, low temperature favors pollutant adsorption.

At the nominal temperature, 25°C, the adsorption time is 70.3 min. At 20°C the adsorption time is 89.4 minutes, an increase of 27%. On the other hand, if the adsorption temperature is 30°C, the adsorption time is reduced to 55.7 min, a reduction of 21%. These results indicate that the adsorption process is very sensitive to the adsorption temperature. A similar observation can be drawn by comparing the pollutant removal rate at different temperatures (see rows 1, 6, and 7 of Table 3).

Desorption Temperature

It can be seen from Table 3 that the desorption process is also very sensitive to temperature. At 80, 70, and 60°C, the desorption times are found to be 9.5, 13.8, and 20.5 min, respectively. Logically, the desorption temperature should be as high as possible. However, the cost of thermal energy and the thermal stability of the bed constrain the maximum desorption temperature.

Pressure

The results reveal that the adsorption time and desorption time are almost inversely proportional to the pressure. However, the fraction of time for the desorption operation is essentially independent of the pressure in the range of operation. The results also show that the capacity per cycle does not change with the pressure. Therefore, the removal rate of the

adsorber is proportional to the pressure. The operating pressure depends on the purpose and situation of operation. From the viewpoint of energy cost, the adsorber should be operated under atmospheric pressure except in a space ship or submarine where a lower or higher pressure prevails naturally.

Superficial Velocity of Gaseous Flow

The value of the linear velocity of gaseous flow given in Table 1 is selected at the adsorption temperature. If the same mass flow rate of air is maintained, the linear velocity during the desorption period is higher than that during the adsorption period because the temperature during the former is higher than that during the latter.

The recommended linear velocities for adsorption fall between 24 and 55 cm/sec (18). The nominal value is chosen to be 40 cm/sec. As shown in Table 3, the adsorption time is relatively longer but the desorption time is only slightly prolonged at a lower velocity. On the other hand, the adsorption time is shortened much more than the desorption time at a higher velocity. Most significantly, the pollutant removal rate is much higher at the higher velocity. A desirable situation is one where the linear velocity is low enough so that the energy for transporting the gas is small and yet is high enough so that the high removal rate is maintained.

Residual Pollutant Loading at the End of Desorption

Lowering of the residual pollutant at the end of desorption prolongs the desorption time. It also prolongs the adsorption time and increases the adsorption capacity. However, in terms of the pollutant removal rate, this does not yield a higher value. As the results in Table 3 indicate, the residual pollutant load should remain reasonably high in order to maintain a high pollutant removal rate.

Extent of Dispersion

Since

$$Pe = GL/\epsilon \rho_g D \quad \text{and} \quad G = u \rho_g$$

the Peclet number can be rewritten as

$$Pe = uL/D\epsilon$$

For the operating conditions under consideration, the Schmidt number is approximately unity and the Reynolds number is in the neighborhood of 100. Under these conditions, the dimensionless group De/ud_p is approximately equal to 0.5 (13), where d_p is the adsorbent particle diameter. Therefore,

$$Pe = \frac{uL}{De} = \frac{ud_p}{De} \frac{L}{d_p} \doteq 2 \frac{L}{d_p}$$

The Peclet number can be perceived as depending only on the adsorber length (bed depth) and the adsorbent particle diameter. The adsorption and desorption times calculated using different Peclet numbers are shown in Table 3. It can be seen that the higher the Peclet number or the less the mixing, the longer the adsorption time. Thus a higher Peclet number is favorable because it requires less frequent desorption. However, a large Peclet number must be achieved by using finer particles and/or a longer adsorber. This gives rise to a higher pressure drop. Furthermore, a large Peclet number does not yield a higher removal rate.

CONCLUDING REMARKS

Two new operational schemes for a single column adsorber system are proposed. The performance of such a system is studied by computer simulation. The results presented here should be useful in designing such an adsorber system. This study also indicates that the single adsorber system can be installed easily and operated effectively. This compact system is especially effective when the limitation of space or weight must be taken into consideration such as in a submarine or space ship.

Acknowledgments

This study was supported by the Environmental Protection Agency (Project No. R-800316). The computer time was provided by the Kansas State University Computing Center.

SYMBOLS

- A cross-sectional area of the adsorber, cm^2
- a available external surface area per unit volume of bed, cm^2/cm^3
- A_1 constant, $(^\circ\text{K})^{1/2}$
- A_2 constant, $^\circ\text{K}$

b adsorption coefficient expressed in the Langmuir isotherm equation
B adsorption coefficient expressed in Eq. (15)
c adsorbate concentration in gas phase, g of adsorbate/g of adsorbate free gas
c* equilibrium concentration, g of adsorbate/g of adsorbate free gas
c_f pollutant concentration, g of adsorbate/g of adsorbate free gas
c_{max} maximum allowable concentration, g of adsorbate/g of adsorbate free gas
D axial dispersion coefficient for mass transfer, cm²/sec
D_a diameter of the adsorber, cm
d_p adsorbent particle diameter, cm
G mass flow rate of fluid per unit cross-sectional area, g of gas/sec-cm²
H_g gas phase hold-up, i.e., mass of gas per unit volume of bed, g of gas/cm³ of bed.
H_s solid phase hold-up, i.e., mass of adsorbent per unit volume of bed, g of adsorbent/cm³ of bed.
K_e dimensionless mass transfer coefficients, $k_e a \rho_g L / G$
k_e external mass transfer coefficient based on external surface of particle and concentration driving force, cm/sec
L depth of adsorber bed, cm
P pressure in the adsorber, atm
Pe Peclet number, $GL/\epsilon \rho_g D$
Q₁ amount of adsorbate loaded on the adsorbent at the end of adsorption, g
Q₂ amount of adsorbate remaining on the adsorbent at the end of desorption, g
 ΔQ $Q_1 - Q_2$, capacity of adsorption, g
q amount of adsorbate adsorbed per unit mass of adsorbent, g of adsorbate/g of adsorbent
q_m amount of adsorbate adsorbed per unit mass of adsorbent, when the adsorbent is fully covered by a monolayer, g of adsorbate/g of adsorbent
T temperature, °K
t time, sec
T_a adsorption temperature, °C
T_d desorption temperature, °C
u superficial linear velocity of gaseous flow, cm/sec

X	dimensionless adsorbate concentration in gas phase, c/c_f
X^*	dimensionless adsorbate equilibrium concentration in gas phase, c^*/c_f
Y	dimensionless adsorbate concentration in solid phase, q/q_m
z	axial distance from top of bed, cm

Greek Letters

α	ratio of adsorbate removal capacity in the gas phase to that in the solid phase in the bed, $H_g c_f / H_s q_m$
β	residual pollutant loading at the end of desorption
ε	void fraction of the bed
λ	dimensionless axial distance, Z/L
ρ_g	density of gas, g/cm ³
ρ_s	density of adsorbent g/cm ³
τ	dimensionless time, tG/LH_g

REFERENCES

1. W. F. Ames, *Numerical Methods for Partial Differential Equations*, Barnes and Noble, New York, 1969.
2. S. Brunauer, *The Adsorption of Gases and Vapors. Volume I. Physical Adsorption*, Princeton University Press, Princeton, New Jersey, 1943.
3. H. T. Chen and F. B. Hill, *Separ. Sci.*, 6, 411 (1971).
4. H. T. Chen, J. L. Rak, J. D. Stokes, and F. B. Hill, *AIChE J.*, 18, 356 (1972).
5. J. A. Danielson (ed.), *Air Pollution Engineering Manual*, U.S. Department of HEW, National Center for Air Pollution Control, Cincinnati, Ohio, 1967.
6. L. T. Fan and S. K. Choi, Institute for Systems Design and Optimization Report No. 41, Kansas State University, Manhattan, Kansas.
7. W. D. Faulkner, W. G. Schuliger, and J. E. Urbanic, Presented at 74th AIChE National Meeting, New Orleans, Louisiana, March 12, 1973.
8. R. A. Gregory and H. H. Sweed, *Chem. Eng. J.*, 1, 207 (1970).
9. R. A. Gregory and N. H. Sweed, *Ibid.*, 4, 139 (1972).
10. R. Gupta and N. H. Sweed, Presented at AIChE National Meeting, Minneapolis, Minnesota, August 29, 1972.
11. J. W. Hessler, *Activated Carbon*, Hill, London, 1967.
12. D. E. Kowler and R. H. Kadlec, *AIChE J.*, 18, 1207 (1972).
13. O. Levenspiel, *Chemical Reaction Engineering*, Wiley, New York, 1962, p. 275.
14. M. M. Mattia, *Chem. Eng. Prog.*, 66, 74 (December, 1970).
15. R. L. Pigford, B. Baker, III, and E. E. Blum, *Ind. Eng. Chem., Fundam.*, 8, 144 (1969).
16. A. C. Stern (ed.), *Air Pollution*, Vol. 3, Academic, New York, 1968.
17. N. H. Sweed and R. H. Wilhelm, *Ind. Eng. Chem., Fundam.*, 8, 221 (1969).
18. R. E. Treybal, *Mass-Transfer Operation*, 2nd ed., McGraw-Hill, New York, 1968.

19. R. H. Wilhelm, A. W. Rice, and A. R. Bendelius, *Ind. Eng. Chem., Fundam.*, 5, 141 (1966).
20. R. H. Wilhelm, A. W. Rice, R. W. Rolke, and N. H. Sweed, *Ibid.*, 7, 337 (1968).

Received by editor June 21, 1975